Reprinted from the

Proceedings of the Eleventh Lunar and Planetary Science Conference

Pergamon Press
New York • Oxford • Toronto • Sydney • Paris • Frankfurt

Proc. Lunar Planet. Sci. Conf. 11th (1980), p. 2031–2041.
Printed in the United States of America

On constraining lunar mantle temperatures from gravity data

Susan Pullan and Kurt Lambeck

Research School of Earth Sciences, Australian National University, Canberra 2600 Australia

Abstract—An estimate of the temperature for the upper lunar mantle is obtained from an inversion of gravity data for density anomalies and the associated stress-state of the moon's interior and the comparison of this stress-state with flow laws and an estimate of likely strain rates. The resulting temperatures are upper limits and at depths of about 300 km, they must be at least 200–300°C less than those proposed by Duba *et al.* (1976) in order to be consistent with the maintenance of lunar gravity anomalies and topography over the past 3–4 billion years.

INTRODUCTION

Estimates of the present-day temperature of the lunar interior are usually based on one or more of the following arguments. (1) An inversion of magnetic data for electrical conductivity profiles (e.g., Dyal *et al.*, 1976) followed by a second inversion for temperature (e.g., Duba *et al.*, 1976; Huebner *et al.*, 1979). Both inversions are non-unique while the latter requires quite crucial assumptions regarding the lunar mantle composition. (2) An interpretation of the two Apollo surface heat flow observations, usually based on a steady state thermal model for the upper mantle (e.g., Keihm and Langseth, 1977). (3) Thermal evolution calculations (e.g., Toksöz *et al.*, 1978), yielding results that are also highly model dependent and that are usually constrained by the observed heat flow data.

Another approach to estimating the lunar temperature is from the present-day stress state of the moon deduced from the lunar gravity and topography observations (Lambeck and Pullan, 1980). The procedure is outlined in Fig. 1 where the principal assumptions associated with each step are also indicated. The observed lunar gravity field indicates the existence of lateral density variations and of a non-hydrostatic stress state. The density structure cannot be determined uniquely from the gravity data alone but the characteristics of the gravitational potential power spectrum point to these anomalies being near the surface, an interpretation that is also in accordance with the correlations seen between gravity and certain topographic features. The second step in the inversion is from density anomalies to stress. An approximate method has been adopted in which

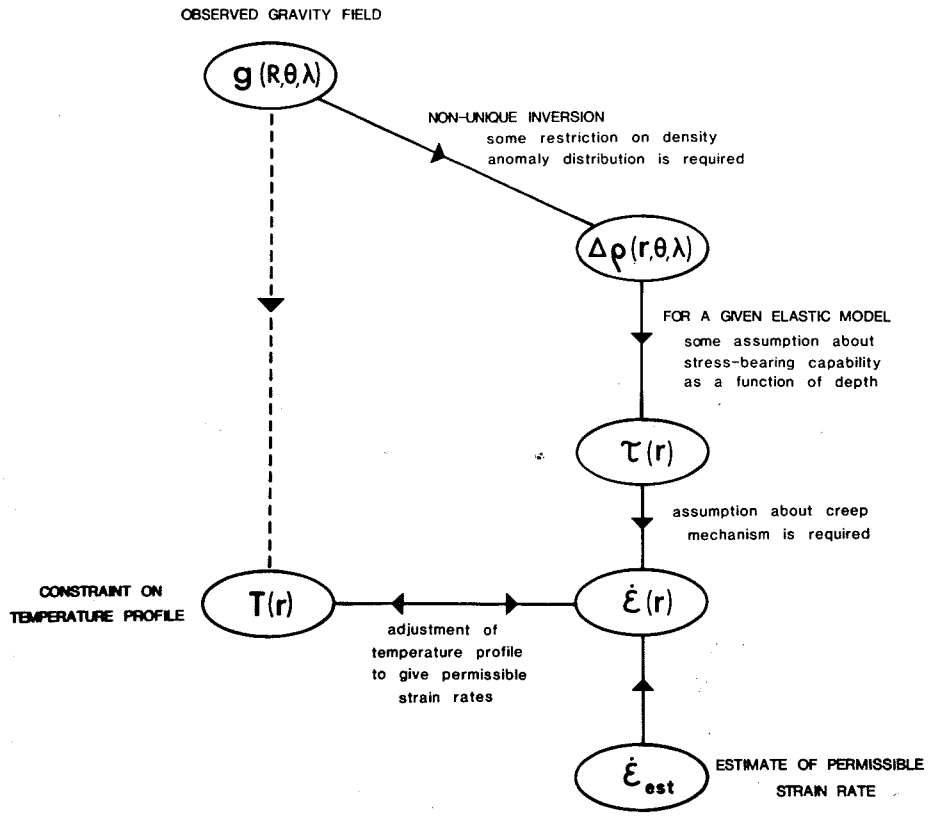

Fig. 1. An outline of the arguments used to arrive at a constraint on the lunar temperature regime from gravity data, with the major assumptions indicated at the appropriate steps.

the moon is modelled as a spherically layered body, initially in a hydrostatic state, and subjected to a surface load deduced from the gravity or from the topography. Seismic data indicate that the outer few hundred km of the moon is fairly homogeneous and characterized by a very high Q. Based on these results and on the evidence that the present day moon does not differ substantially from the moon of 3 AE ago, the stress state is calculated for a number of simple two-layer models with elastic "lithospheres" of varying thicknesses overlying an inner region that is too weak to support any significant stress-differences. The resulting stress profiles are then inverted for strain-rates using flow laws for dry olivine. These flow laws and consequently the strain-rates are strongly temperature dependent and, together with an estimate of the total strain that the moon has experienced, provide a limit to the present day lunar temperature profile. In this paper the same approach is used with the emphasis being on the assumptions that have been made and the consequence of these assumptions on the deduced selenotherm. The main result is that the temperatures in the upper regions of the

moon may be considerably lower, by some 200–300°C, than given by the conductivity models of Duba *et al.* (1976), and at or below the lower limits given by Keihm and Langseth (1977).

THE OBSERVATIONAL EVIDENCE

Phillips and Lambeck (1980) discuss the observational evidence for the lunar gravity field. The anomalous gravitational potential at selenocentric distance r, latitude ϕ and longitude λ is expressed as a series of spherical harmonics

$$\Delta U(r,\phi,\lambda) = \frac{GM}{r}\sum_{l=2}^{\infty}\left(\frac{R}{r}\right)^{l}\sum_{m=0}^{l}(\bar{C}_{lm}\cos m\lambda + \bar{S}_{lm}\sin m\lambda)\bar{P}_{lm}(\sin\phi) \qquad (1)$$

where $\bar{P}_{lm}(\sin\phi)$ are fully normalized Legendre polynomials, $\bar{C}_{lm}$ and $\bar{S}_{lm}$ are the corresponding Stokes co-efficients, R is the lunar radius, M is the mass of the moon and G is the gravitational constant. The dimensionless power spectrum of the gravitational potential is defined by

$$V_l^2(\Delta U) = \sum_{m}(\bar{C}_{lm}^2 + \bar{S}_{lm}^2). \qquad (2)$$

The relatively slow decay of this power spectrum with increasing degree l is consistent with a model of near surface density anomalies of short wavelength. This does not preclude the existence of lateral density variations at greater depth but these must be relatively small for otherwise the decay of the spectrum would be more rapid.

The anomalous near-surface density layer $\sigma_g(\phi,\lambda)$ can also be expanded in spherical harmonics and its power spectrum is related to the potential spectrum according to

$$V_l^2(\sigma_g) = \left(\frac{2l+1}{3}\right)^2(\bar{\rho})^2\,V_l^2(\Delta U) \qquad (3)$$

where $\bar{\rho}$ is the mean density of the moon. The average crustal density is denoted by ρ_c. The surface load due to the observed lunar topography is $\sigma_t(\phi,\lambda) = \rho_c h(\phi,\lambda)$ and has a power spectrum of

$$V_l^2(\sigma_t) = (\rho_c)^2 V_l^2(h) \qquad (4)$$

where $V_l^2(h)$ is the power spectrum of the observed topography. According to Bills (1978), a smoothed estimate of this spectrum is

$$V_l^2(h) = 1.5 \times 10^{-6}/l(l+1). \qquad (5)$$

Comparing the two estimates σ_g and σ_t of the near-surface load leads to $\sigma_t > \sigma_g$, indicating that the topography is at least partly isostatically compensated. In the following discussion the two surface density layers σ_g and σ_t are used as measure of the load stressing the moon.

An approximate method has been adopted for calculating the stress-differences

set up in an elastic sphere due to a harmonic surface load σ_g or σ_t. In keeping with the statistical approach, the maximum stress-difference $\tau_{lm}(r)$ is computed for each harmonic and is averaged over a spherical surface of radius r. The average maximum stress-difference due to a number of harmonics is given by

$$\bar{\tau}(r) = \left\{ \sum_l \sum_m \tau_{lm}^2(r) \right\}^{\frac{1}{2}}. \tag{6}$$

These stress-differences reflect the conditions in the body below the load, while the stress-differences near the surface due to the topography will be of the order of ρgh. At any point on the shell of radius r the maximum stress-difference may exceed the value given by Eq. (6) and a reasonable upper limit is obtained by

$$\tau_{max} \simeq \sum_l \sum_m \tau_{lm}(r) \tag{7}$$

which may exceed the estimate Eq. (6) by a factor of about four. In Lambeck and Pullan (1980) the stress values that are given are inadvertently referred to as stress-differences whereas they actually are shear-stresses. Hence all stress-difference estimates given in that paper should be increased by a factor of 2.

The stresses associated with each harmonic in the surface load have been estimated from the average distortional strain energy E_s (see, for example, the formulation by Kovach and Anderson, 1967) according to $\tau \simeq (8/3)(\mu E_s)^{\frac{1}{2}}$ where μ is the rigidity. By using the methods developed by Kaula (1963) and applied to the moon by Arkani-Hamed (1973) it is possible to carry out a more rigorous inversion of gravity for both density anomalies and deviatoric stresses without going through the surface layer representation but, in view of the evidence that the density anomalies are mainly surficial, this is not warranted for the present purpose.

The magnitude and distribution of the stress-differences beneath the surface load depend on the elastic properties of the body. In constructing the models used for these calculations we have been guided largely by the seismic evidence. Published seismic models all indicate an upper mantle of a few hundred km that is characterized by an extremely high shear Q. Below ~300 km (Nakamura *et al.*, 1976), or perhaps 500 km (Goins *et al.*, 1978), and extending to depths of ~1000 km the Q may be reduced but it is still much higher than for the earth's upper lithosphere. These high Q values suggest that the lunar mantle is volatile-poor and that partial melting is not widespread. The occurrence of moonquakes at depths of ~800 km is further supporting evidence for a relatively cold and thick lunar lithosphere. On this basis, the average stress-differences have been computed for a series of models having elastic lithospheres of 1000 km, 500 km, 400 km and 300 km thicknesses (see Fig. 2). Thus the thickness of the tectonic lithosphere is estimated to be from 30 to 100% of that of the seismic lithosphere. If an analogy with the earth is valid, then 30–50% of the seismic thickness appears as a reasonable choice. The distribution of the stress-differences with depth varies according to the degree of the load—the low degree loads tend to stress the

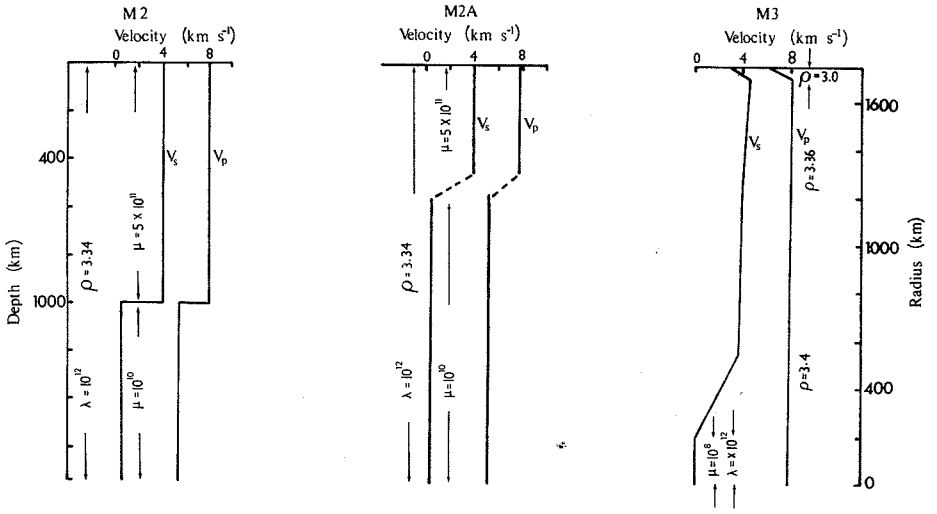

Fig. 2. The variation of elastic parameters with depth for the models considered in this work (units for λ, μ, ρ in cgs). Models M2B and M2C are equivalent to M2A, except that in these models the transition layer is centred at a depth of 400 km and 300 km respectively.

interior while higher degrees of the load stress mainly the layers close to the surface. If the deeper regions of the body are incapable of supporting such stresses, the low degree components of the stress-differences become concentrated in the outer elastic "lithosphere" just above the rigidity interface.

Figure 3 illustrates $\bar{\tau}(r)$ for five different spherical models (Fig. 2) loaded at their surfaces by the density layer σ_g. Only harmonics up to degree 12 have been considered as these loads are the dominant contributors to the stress-differences in the lower regions of the elastic lithosphere. The results in Fig. 3 demonstrate two points: first, that the stress-difference profiles become highly peaked as the stress-bearing lithosphere is thinned, and second, that the magnitude of the stress-differences is only of the order of a few tens of bars with the estimate of an upper limit [τ_{max} as defined in Eq. (7)] approaching perhaps 200 bars. These values are compatible with those obtained by Arkani-Hamed (1973) and also with the lack of evidence of any significant tectonic activity on the lunar surface. For the surface load σ_t, the stress-differences in the lunar interior are approximately twice those illustrated here if there is no isostatic compensation. To obtain an estimate of the contributions of the higher degree harmonics, the topographic spectrum can be used to estimate $\tau \approx \rho gh$

$$\tau_{(l>12)} \approx \rho_c g R \sqrt{\sum_{l=13}^{\infty} V_l^2(h)}.$$

With Eq. (5) this leads to an estimate of $\tau_{(l>12)} \approx 30$ bars, and the higher degree terms ($l > 12$) of the load can be justifiably ignored.

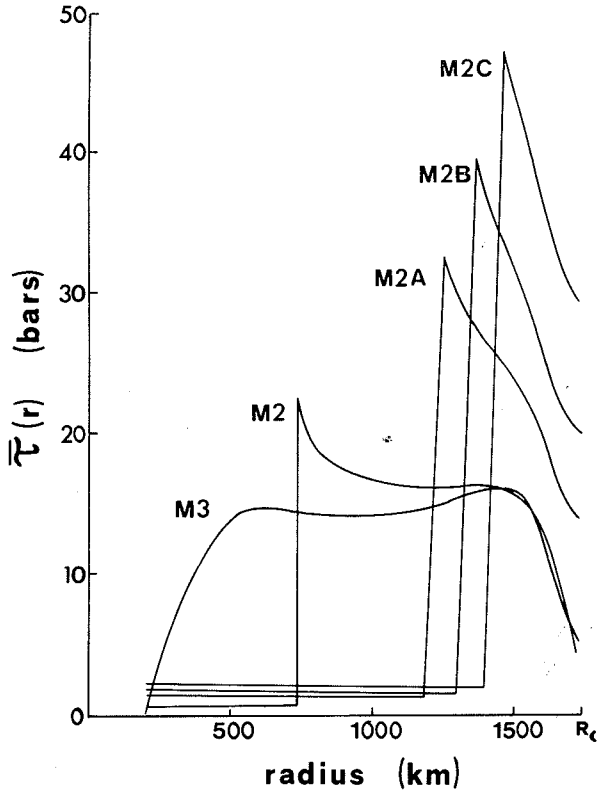

Fig. 3. Stress-differences as a function of depth evaluated according to Eq. 6, for the lunar models described in Fig. 2.

Strain rates in the mantle will in general be stress, temperature and pressure dependent and the following power law is adopted,

$$\dot{\epsilon} = A\tau^n \exp(-(E^* + PV^*)/RT)$$

where $\dot{\epsilon}$ is the strain rate, E^* and V^* are the activation energy and volume, R is the gas constant, P is the pressure and T the temperature. The constants A and n and the parameters E^* and V^* depend on the chemical and mineralogical composition of the material as well as on the mechanisms that dominate the creep process. For a given distribution of temperature with depth this flow law permits the calculated stress-differences given in Fig. 3 to be converted to strain rates in the lunar mantle. For the moon, $PV^* \ll E^*$ and the choice of the activation volume is not critical. However, the choice of E^* and n is critical for, with the stress-differences, temperatures and pressures considered here, a change in E^* of only 10% results in a change in the strain rate of three orders of magnitude. The strain rate profiles have been calculated using experimentally derived flow laws for dry olivine and the validity of the results depends critically on two

assumptions: that dry olivine is an appropriate model of the lunar interior, and that the flow laws can be extrapolated from laboratory to geological conditions. Certainly the lunar mantle is not composed exclusively of olivine, but probably also contains pyroxenes, garnet, etc. Goetze (1978) did not consider that such a mixture would significantly effect the creep strength of the material but experimental data on the creep of pyroxenes is sparse. The extrapolation of laboratory determined rheologies to geological problems is unavoidable in many areas of the geological and geophysical sciences if any progress is to be made at all, yet it is fraught with problems. In laboratory experiments loading cycles are short and the measured strain rates are very fast compared to those acting on geologic time scales. Hence any extrapolation to geological problems remains extremely uncertain. However, it can be expected that on geological time scales, creep will become significant at much lower temperatures than in the laboratory (Carter, 1976), and that secondary creep mechanisms not observed on a short time scale may become operative (Paterson, 1976). Thus strain rates calculated from the experimentally derived flow laws could be considered as lower limits. Several flow laws for dry olivine have been published (e.g., Kirby and Raleigh, 1973; Durham and Goetze, 1977; and Post, 1977) and, when applied to the stress-difference profiles given in Fig. 3, give strain rates that vary over three or four orders of magnitude. Only Post's (1977) rheology, which results in the lowest calculated strain rates, will be considered here. The other rheologies will lead to higher strain rates and hence require lower temperatures if the stresses are to be maintained. For the selenotherm based on the inversion of electrical conductivity profiles by Duba *et al.* (1976) (see Fig. 4), Post's rheology and the stress-difference profiles (Fig. 3) for the models given in Fig. 2 lead to strain rates in the elastic lithosphere that are of the order of 10^{-16} sec^{-1} (Fig. 5).

Present strain rates on the moon are not observable, but the general absence of major tectonic activity over the last 3 AE would imply low values. It appears that by late Pre-Imbrian time the crust and upper mantle temperatures were probably low enough for subsequent isostatic readjustments to be small. The following period, Imbrian time, was characterized by the basaltic volcanism which led to the formation of the mass concentrations in the near side circular maria. These mascons do not appear to have reached an isostatic balance although the concentric graben structures and compressional wrinkle ridges point to a mild form of tectonic failure at the surface (see Phillips and Lambeck, 1980 for a further discussion).

A measure of total strain since the time of the last major bombardment of the lunar surface may be deduced from the present lunar topography spectrum and Lambeck and Pullan (1980) estimated an average strain rate of 10^{-19}–10^{-21} sec^{-1}. Solomon and Chaiken (1976) argue that the absence of surface features that can be attributed to planetary changes in volume, leads to the constraint that the lunar radius has changed by no more than 1 km since the emplacement of the oldest mare surfaces 3.8 AE ago. This constraint also points to an average strain rate over the last 3–4 AE of the order of 10^{-20} sec^{-1}. These values would be upper limits to present day strain rates since any major relaxation would have occurred early in this time period.

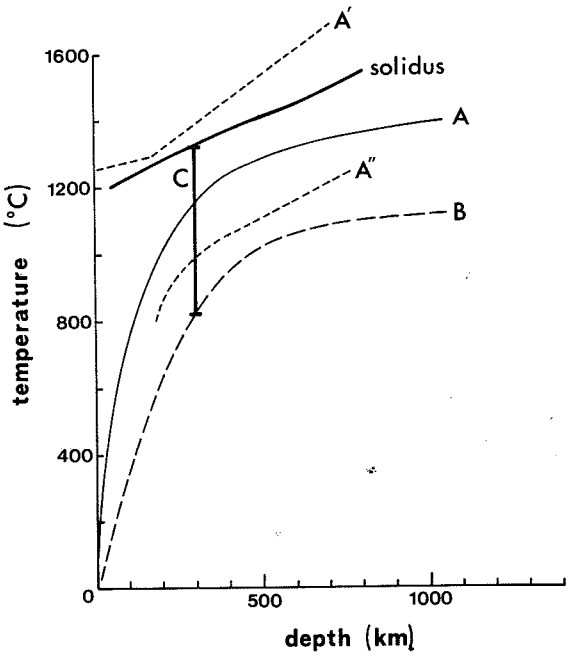

Fig. 4. Estimates of the selenotherm according to
A) Duba *et al.* (1976)
B) this work
C) Keihm and Langseth (1977)

IMPLICATIONS

The strain-rates calculated using Duba *et al.*'s (1976) selenotherm clearly exceed the estimated upper limits of the present day values for all models considered (see Fig. 5) but before drawing any conclusions it may be useful to reiterate some of the consequences of the assumptions made in obtaining these values. First, density anomalies may, and undoubtedly do, occur below the upper mantle and crustal layer to which they have been restricted in the inversion. Hence the stress and strain-rates may be underestimated. Second, the manner in which stresses due to individual spherical harmonics in the load are summed leads to average values for the maximum stress-difference but maximum values may exceed these by a factor of 4 (compare the expressions 6 and 7). Third, if an uncompensated topography is taken to be the load the stress differences may be further underestimated by a factor of about 2. Since strain-rate is proportional to (stress-difference)^3 these three points indicate that the results in Fig. 5 could be underestimated by as much as three orders of magnitude. Fourth, the extrapolation of the flow laws to geological conditions may lead to an underestimation of the

calculated strain-rates while the "observed" strain-rates represent upper limits.

Taken together, the discrepancy between the computed and "observed" strain-rates may be even greater than indicated in Fig. 5 and this implies that the stress-differences should have relaxed and that much of the topography and gravity anomalies should have vanished during the last 4 billion years. One way to avoid this is to lower the selenotherm. No attempt has been made here to carry out a formal inversion for temperature, but we have introduced a rather *ad hoc* upper limit for lunar mantle temperatures (Fig. 4) on the basis that it leads to "acceptable" strain rates. The essential point is that the temperature near 300 and 400 km depth must be at least 200–300°C less than that proposed by Duba *et al.* (1976)—that is, at or below the lower limit suggested by Keihm and Langseth (1977) and similar to the present day temperatures proposed by Toksöz *et*

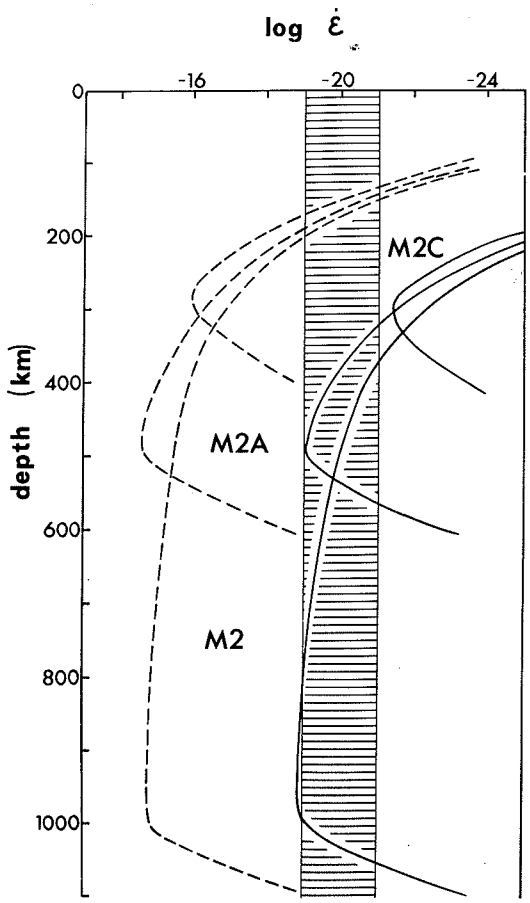

Fig. 5. Strain rates calculated using Post's (1977) rheology and the stress-difference profiles of Fig. 3—for the nominal temperature profile B (solid lines) and Duba *et al.*'s (1976) selenotherm (dashed lines).

al. (1978). This conclusion appears unavoidable unless the extrapolation of the laboratory-determined flow laws to lunar conditions is entirely inappropriate.

The above arguments for a relatively cool moon are for the present-day, although it is implied that the moon has not undergone any significant thermal evolution for the last 3 AE. This is contradictory to the thermal evolution model proposed by Toksöz *et al.* (1978) in which the lithosphere was less than 100 km thick 4 AE ago and would have increased to only a little more than 100 km by 3.2 AE ago. The high selenotherms proposed by Toksöz *et al.* for the period of mare formation require that the relatively thin and warm lithosphere can support considerably greater stress-differences than those estimated to exist in the moon now, for not only will there have been some relaxation of stress, but the stress-differences would have been concentrated in a much thinner layer. The present calculations are not very helpful in the case of a thin lithosphere since deformation will be controlled by the brittle strength of the crustal material rather than by the creep strength. Solomon and Head (1979) used a model of a thin spherical elastic shell overlying a fluid interior to compute the stresses in the lithosphere due to mascon loading, and obtained stress-differences of the order of 0.5–1 kbar. These are, however, lower limits for two reasons. They consider the present load, not that at the time of mascon formation, and they have not considered the low degree harmonics in the load, though it is these that most stress the shell (see Lambeck and Pullan, 1980). Kuckes (1977) has considered he overall non-equilibrium figure of the moon (i.e., the second degree harmonics), and estimated that these alone would produce stresses of the order of 400 bars in a 100 km thick elastic shell.

Arkani-Hamed (1974) concluded that the thickness of the lunar lithosphere had to be about 400 km at the time of the formation of the Serenitatis mascon to support the associated stress-differences, which he estimates are presently around 70 bars; a conclusion that is in accord with the present study. More recently Delano *et al.* (1980) have argued that the mare basalts originated at depths of 400 to 500 km, a further indication that in the interval 3.9–3.2 AE ago the lithosphere may have been thicker by a factor of about 4 than assumed by Toksöz *et al.*, and that the subsequent thermal evolution of the upper part of the lunar mantle has been less important than suggested by their model.

REFERENCES

Arkani-Hamed J. (1973) Density and stress distribution in the moon. *The Moon* **7**, 84–126.

Arkani-Hamed J. (1974) Stress constraint on the thermal evolution of the moon. *Proc. Lunar Sci. Conf. 5th*, p. 3127–3134.

Bills B. G. (1978) A harmonic and statical analysis of the topography of the Earth, Moon and Mars. Thesis, California Institute of Technology, Pasadena. 263 pp.

Carter N. L. (1976) Steady state flow of rocks. *Rev. Geophys. Space Phys.* **14**, 301–360.

Delano J. W., Taylor S. R., and Ringwood A. E. (1980) Composition and structure of the deep lunar interior (abstract). In *Lunar and Planetary Science X*, p. 225–227. Lunar and Planetary Institute, Houston.

Duba A., Heard H. C., and Schock R. N. (1976) Electrical conductivity of orthopyroxene to 1400°C and the resulting selenotherm. *Proc. Lunar Sci. Conf. 7th,* p. 3173–3181.

Durham W. B. and Goetze C. (1977) Plastic flow of oriented single crystals of olivine. I. Mechanical data. *J. Geophys. Res.* **82,** 5737–5753.

Dyal P., Parkin C. W., and Daily W. D. (1976) Structure of the lunar interior from magnetic field measurements. *Proc. Lunar Sci. Conf. 7th,* p. 3077–3095.

Goetze C. (1978) The mechanisms of creep in olivine. *Phil. Trans. Roy. Soc. London* **A288,** 99–119.

Goins N. R., Toksöz M. N., and Dainty A. M. (1978) Seismic structure of the lunar mantle: An overview. *Proc. Lunar Planet. Sci. Conf. 9th,* p. 3575–3588.

Huebner J. S., Duba A., and Wiggins L. B. (1979) Electrical conductivity of pyroxene which contains trivalent cations: Laboratory measurements and the lunar temperature profile. *J. Geophys. Res.* **84,** 4652–4656.

Kaula W. M. (1973) Elastic models of the mantle corresponding to variations in the external gravity field. *J. Geophys. Res.* **68,** 4967–4978.

Keihm S. I. and Langseth M. G. (1977) Lunar thermal regime to 300 km. *Proc. Lunar Sci. Conf. 8th,* p. 499–514.

Kirby S. H. and Raleigh C. B. (1973) Mechanisms of high-temperature, solid state flow in minerals and ceramics and their bearing on the creep behaviour of the mantle. *Tectonophys.* **19,** 165–194.

Kovach R. L. and Anderson D. L. (1967) Study of the energy of the free oscillation of the earth. *J. Geophys. Res.* **72,** 2155–2168.

Kuckes A. F. (1977) Strength and rigidity of the elastic lunar lithosphere and implications for present-day mantle convection in the moon. *Phys. Earth Planet. Inter.* **14,** 1–12.

Lambeck K. and Pullan S. (1980) Inferences on the lunar temperature from gravity, stress state and flow laws. *Phys. Earth Planet. Inter.* **22,** 12–28.

Nakamura Y., Latham G. V., Dorman H. J., and Duennebier F. K. (1976) Seismic structure of the moon: A summary of current status. *Proc. Lunar Sci. Conf. 7th,* p. 3113–3121.

Paterson M. S. (1976) Some current aspects of experimental rock deformation. *Phil. Trans. Roy. Soc. London* **A283,** 163–172.

Phillips R. J. and Lambeck K. (1980) Gravity fields of the terrestrial planets: Long wavelength anomalies and tectonics. *Rev. Geophys. Space Phys.* **18,** 27–77.

Post R. L. (1977) High-temperature creep of Mt. Burnet dunite. *Tectonophys.* **42,** 75–110.

Solomon S. C. and Chaiken J. (1976) Thermal expansion and thermal stress in the moon and terrestrial planets: Clues to early thermal history. *Proc. Lunar Sci. Conf. 7th,* p. 3229–3243.

Solomon S. C. and Head J. W. (1979) Vertical movement in mare basins: Relation to mare implacement, basin tectonics, and lunar thermal history. *J. Geophys. Res.* **84,** 1667–1682.

Toksöz M. N., Hsui A. T., and Johnston D. H. (1978) Thermal evolutions of the terrestrial planets. *Moon and Planets* **18,** 281–320.